Research on Detection Method of Corrosion Residual Wall Thickness in Pipeline of Oil and Gas Gathering and Transportation

Chunlin Cheng[1, a], Mingjiang Shi

[1]Southwest Petroleum University, Chengdu, 610500, China.

[a]ksmomo110@163.com

Abstract

The oil and gas gathering station includes metering stations, oil transfer stations, dehydration stations, etc. As an important petroleum transportation hub, the amount of crude oil passed and processed every day is very large, and the crude oil contains various corrosive liquids and corrosive gas components. The erosion and corrosion of the corrosive mixed liquid on the wall of the station process is the main form of pipeline failure. Pulse eddy current detection technology is widely used in the field of non-destructive testing because of its wide spectrum, strong penetrating power, no need for coupling agent and the ability to realize on-line rapid detection. In this paper, the pulse eddy current testing technology is studied for the wall thinning caused by corrosion. The pulse eddy current testing technology is analyzed by the circuit transition process theory and the pulse eddy current theory. The pulse eddy current testing technology is theoretically analyzed. The finite element model of pulsed eddy current testing was built. The multi-physics finite element simulation software COMSOL was used to simulate the relationship. The proportional relationship between the depth of the defect and the phase change of the magnetic field signal was obtained. The far-field eddy current was confirmed to the inner and outer wall defects. Consistent detection sensitivity.

Keywords

Pulse eddy current; Oil and gas gathering; Residual wall thickness.

1. Introduction

Pipeline transportation is currently the most scientific and convenient transportation method. Due to the flammable and explosive nature of oil and natural gas, pipeline transportation is carried out in an air-insulated environment, which greatly reduces the possibility of explosions caused by transportation, and the oil and gas during transportation is not like traditional The transportation method is the same because of frequent operation, which is a relatively safe safety rate, less loss, and more environmentally friendly transportation. In addition, the transportation pipeline is generally buried underground, reaching as much as 94% of the total length of the pipeline. Compared with the construction of road transportation, it not only occupies less land area, but also has lower cost, and the transportation process is less susceptible to external natural conditions and other factors. The impact of continuous and efficient transportation can greatly improve transportation efficiency and economic efficiency compared with traditional transportation methods.

With the gradual increase of oil and gas pipelines, the number of joint stations in the oil gathering and transportation process has also increased. As an important hub in the entire petroleum system, the oil and gas gathering and transportation station serves as a collection of crude oil and natural gas. Tasks such as storage, processing, and transportation are characterized by complex piping arrangements, relatively small pipe diameters, and variable

media, including water, oil, gas, and various mixed media. Compared with the long-distance pipeline, due to the diversity of the medium in the station process pipeline, it is more susceptible to internal corrosion damage. In addition, under the joint action of internal defects of the pipe body and external environment changes, the process pipeline will be different. The degree of damage and corrosion will become an important factor threatening the safety of oil and gas gathering and transportation stations. Therefore, it is of great significance to study the residual wall thickness detection method of station process pipeline corrosion.

2. Theoretical Analysis of Defect Detection in Far Field Eddy Current Pipeline

There are many types of detection technologies in the field of electromagnetic detection technology, and far-field eddy current detection technology is one of them. Far-field eddy current is a special type of eddy current detection technology. It is different from conventional eddy current. It uses the unique properties of eddy-field far-field region to carry out defect detection tasks. This chapter analyzes the theory of far-field eddy current pipeline defect detection and derives far. A mathematical model of electromagnetic propagation of a field vortex inside an oil and gas pipeline.

2.1. Principle of Far Field Eddy Current Testing Technology

The pipeline defect detection probe based on far field eddy current technology is generally built-in type. The far field eddy current is a low frequency eddy current detection technology that can penetrate the metal tube wall twice. The detection principle is shown in Figure 1. The main structure of the far field eddy current probe includes an excitation coil placed coaxially with the pipeline to be tested and a detection coil placed in the far field region, and some parts for improving the detection performance of the probe, such as a shielding device, a magnetic guiding device, a magnetic saturation device, etc.

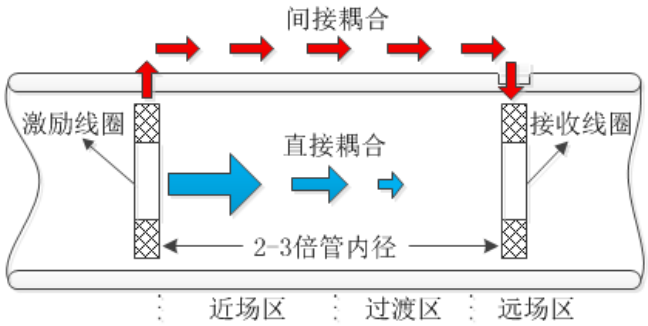

Fig 1. Schematic diagram of far field eddy current defect detection

After the low-frequency sinusoidal alternating current is applied into the excitation coil, three typical far-field eddy currents in the near-field region, the transition region and the far-field region are formed in the pipeline, and a direct energy flow path appears in the tube, and energy is generated near the tube wall. Indirect flow path. In the near-field region, the alternating magnetic field generated by the excitation coil is strong, but as the axial distance from the excitation coil increases, the magnetic field strength is drastically attenuated to a minimum due to the shielding effect of the induced eddy current in the wall near the excitation coil. The magnetic field distribution in this region cannot contribute to the defect detection signal; the far field region is meaningful for the defect identification. The excitation coil and its adjacent tube wall form a transformer structure, and a circumferential eddy current is generated in the tube wall, and a part of the eddy current rapidly diffuses. To the outer surface of the tube, these circumferential eddy currents generate an alternating magnetic field that diffuses into the air

near the wall of the tube and conducts along the tube to the far field. The indirect energy in the far field is much larger than the direct energy, so the magnetic field outside the tube Passing through the pipe wall again into the far field, the far field magnetic field passing through the two pipe walls contains the wall defect information, which can be identified by the detection coil and found defects; although the transition zone magnetic field does not help the defect detection, the transition zone will appear. In the magnetic valley, the magnitude and phase of the magnetic induction intensity will have large transitions, which are unique phenomena of the far field eddy current.

The magnitude of the induced voltage output from the signal receiving coil and the phase difference with the excitation voltage vary as the distance between the receiving coil and the exciting coil increases, as shown in Figure 2. In the figure, Di represents the pipe inner diameter value.

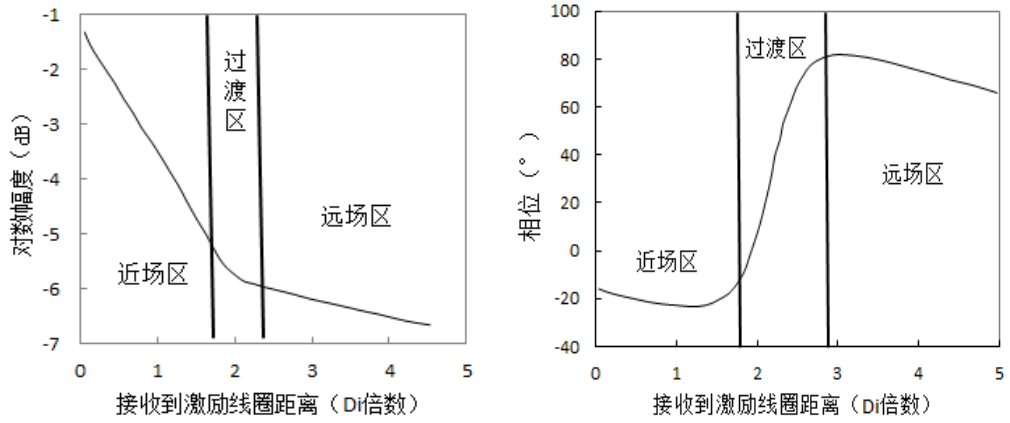

(a) Amplitude characteristic curve (b) Phase characteristic curve

Fig 2. Detection signal-distance relationship curve

It can be seen from the amplitude and phase characteristic curves in Figure 2 that in the near-field, transition and far-field regions of the far-field eddy, the amplitude and phase curves show different variations. In the near-field region within about 1.8 times the inner diameter of the tube from the excitation coil, the induced potential value of the receiving coil is rapidly attenuated, and the phase difference between the detected signal voltage and the excitation voltage remains substantially unchanged. In the transition zone from the excitation coil about 2 times the inner diameter of the pipe, the amplitude of the detection signal induced potential is attenuated at a small speed, and the phase difference changes greatly. In the far field region, which is about 3 times the inner diameter of the tube from the excitation coil, the amplitude and phase of the induced voltage change with a slow tendency.

The far-field detection signal can be approximated by a one-dimensional skin effect formula compared to the phase lag of the excitation signal:

$$\theta=2\mathrm{h}\sqrt{\pi f\mu\sigma} \tag{1}$$

In the above formula, the phase lag of the induced potential is the measured wall thickness, and the excitation frequency is the permeability of the material of the pipe wall, which is the electrical conductivity of the pipe wall material.

It can be seen from the formula (1) that the two factors except the phase difference between the excitation signal and the detection signal and the thickness of the wall to be tested are unknown, and other parameters can obtain specific values. Therefore, when using the far-field eddy current to detect the pipeline defect, as long as the phase information of the detection

signal is obtained, the thickness information of the pipe wall can be estimated, and then the normal wall thickness can be compared to determine whether the pipe wall is defective.

2.2. Far Field Eddy Current Pipeline Defect Detection Mathematical Model

Far-field eddy current is a low-frequency electromagnetic field detection technology, and low-frequency can be regarded as a super-stable superposition. Therefore, it is only necessary to observe its steady-state characteristics, so the following assumptions are made:

(1) Current density J and field quantity E, D, B, H, etc. change with sinusoidal law over time, and their influence on harmonic components is negligible;

(2) The influence of the speed of the probe on the magnetic field and eddy current can be neglected;

(3) The parameters in the model are isotropic and constant;

(4) The hysteresis effect is 0;

(5) Displacement current is 0

Based on the above assumptions, the quasi-steady-state Maxwell equations are obtained:

$$\begin{cases} \nabla \times H = J_c + J_e \\ \nabla \times E = -j\omega B \\ \nabla \cdot B = 0 \\ \nabla \cdot D = \rho \end{cases} \tag{2}$$

H is the magnetic field strength, B is the magnetic induction intensity, D is the electric displacement vector, E is the electric field strength, ρ the body current density, J_c is the applied excitation current density, and J_e is the eddy current density. The relationship between them is determined by the nature of coal. For isotropic coal, the theory of magnetic fields is:

$$D = \varepsilon E \ , \ B = \mu H \ , \ J_e = \sigma E \tag{3}$$

To facilitate the simplification and numerical calculation of the equations, the vector magnetic potential is defined and is defined by the Coulomb specification:

$$\nabla \times A = B \tag{4}$$

$$\nabla \cdot A = 0 \tag{5}$$

Substituting the formula (4) into the formula (2) can be obtained:

$$\nabla \times (E + j\omega A) = 0 \tag{6}$$

Define the scalar potential function based on the spinlessness:

$$E + j\omega A = -\nabla \varphi \tag{7}$$

Then:

$$E = -(\nabla\varphi + j\omega A) \tag{8}$$

Substituting equations (3), (4), and (8) into Maxwell's equations (2) are:

$$\nabla \times [\frac{1}{\mu}(\nabla \times A)] = J_c - \sigma(\nabla\varphi + j\omega A) \tag{9}$$

From the isotropic nature of the material, and according to the Coulomb specification and vector equations are:

$$\nabla^2 A = -\mu J_c + \mu\sigma(\nabla\varphi + j\omega A) \tag{10}$$

The Maxwell equation has:

$$\nabla \times J = -\frac{\partial\rho}{\partial t} \tag{11}$$

Substituting the formula (8) into the formula (11) can be obtained:

$$-\nabla\bullet\sigma(\nabla\varphi + j\omega A) = -\frac{\partial\rho}{\partial t} \tag{12}$$

Ignore the displacement current, then, isotropic and constant, then:

$$\nabla\bullet(\nabla\varphi + j\omega A) = 0 \tag{13}$$

Given the boundary conditions, the sum of the equations (10) and (13) is calculated, and further:

$$B = \nabla \times A \tag{14}$$

$$J_e = -\sigma(\nabla\varphi + j\omega A) \tag{15}$$

The mathematical model of the far-field eddy current in cylindrical coordinates is:

$$\frac{\partial^2 A_\theta}{\partial r^2} + \frac{1}{r}\frac{\partial A_\theta}{\partial r} + \frac{\partial^2 A_\theta}{\partial z^2} - \frac{A_\theta}{r^2} = -\mu J_{c\theta} + j\omega\mu\sigma A_\theta \tag{16}$$

A_θ Can be solved by formula (16), and further can be obtained:

$$B_r = -\frac{\partial A_\theta}{\partial Z}$$
$$B_z = \frac{A_\theta}{r} + \frac{\partial A_\theta}{\partial r} \quad (17)$$
$$J_{e\theta} = -j\omega\sigma A_\theta$$

3. Finite Element Simulation of Far Field Eddy Current Pipeline Defect Detection

Finite element simulation is a necessary part of the development of various scientific research projects since the beginning of the new century. The study of electromagnetic field phenomena is a powerful analytical tool. Based on the analysis of the mathematical model of far-field eddy current pipeline defect detection in the previous chapter, this chapter uses the finite element simulation software COMSOL Multiphysics as a tool to carry out simulation experiments on the full-circumference axisymmetric defect of the far-field eddy current in the pipeline and the relationship between the internal and external wall defect signals. the study.

3.1. Full-Circumferential Axisymmetric Defect Detection Simulation

In the simulation model, a defect is established on the outer wall of the pipe far from the inner tube of the inner tube of the excitation tube, as shown in Figure 3. The parameters such as the outer diameter and inner diameter of the pipe are kept consistent with the previous simulation model, except that the groove defect shown in the figure is established on the outer wall of the far-field pipe. The defect is a full-circumferential axis-symmetric defect, so on the upper and lower pipe walls of the schematic A defect with the same parameters has appeared. The defect width is 5mm, and the depth is set to 1mm, 2mm, 3mm and 4mm. The influence of the depth variation of the defect on the magnetic field signal is mainly studied.

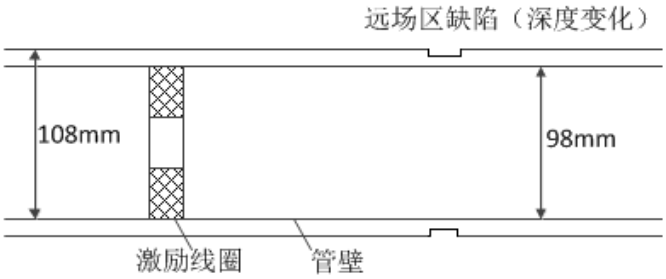

Fig 3. Schematic diagram of defect formation in far field

Firstly, the change of the magnetic field signal under the 3mm depth defect is analyzed. The far-field eddy current simulation model of the defect is calculated to obtain the magnetic field line distribution near the defect, as shown in Figure 4.

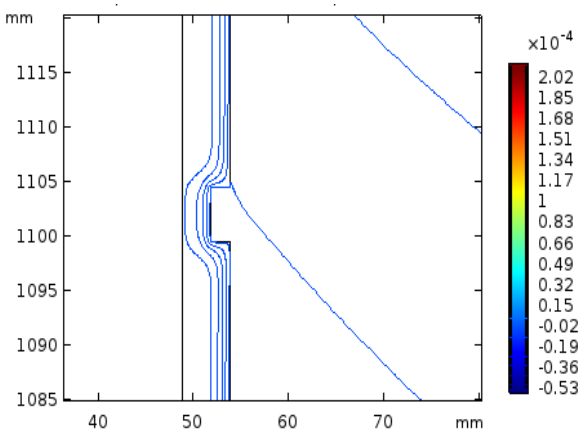

Fig 4. Magnetic field line map near the defect

It can be seen from the magnetic field line distribution diagram near the defect in Fig. 4 that in the presence of the defect, the magnetic field line bends around the defect. This means that when there is a defect in the tube wall, the magnetic field near the defect changes, and the magnetic induction intensity also changes. When the detecting coil reaches the defective pipe section from the non-defective pipe section, a change in the magnetic induction intensity is sensed, and the output voltage of the detecting coil also changes, thereby detecting the existence of the defect.

In the presence of defects, the simulation results show that the axial component Bz amplitude and phase of the magnetic induction intensity near the inner wall of the pipe (within 10 mm) are gradually away from the excitation coil with the detection point, as shown in Figure 5. When there is a defect in the tube wall, the amplitude and phase curves of the excitation tube are doubled at the inner diameter of the tube, indicating that the amplitude and phase of Bz have changed. At the same time, it can be found that only in the small range near the defect, the amplitude and phase of Bz change, and the curve does not change slightly away from the defect. This shows that the defect only affects the magnetic field in a small area nearby, and the detection coil senses this small range of magnetic field changes to find the defect.

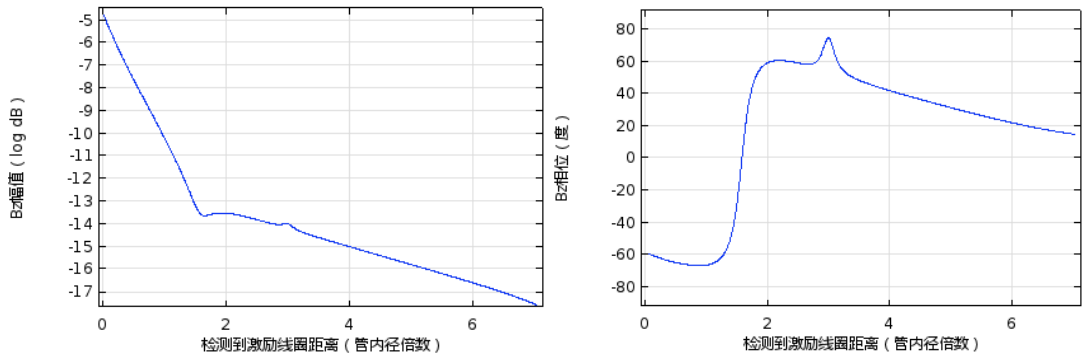

(a) Bz amplitude variation curve under defects (b) Bz phase change curve under defect

Fig 5. Bz amplitude and phase curve

3.2. Analysis of Comparison Results of Different Depth Defect Detection Simulations

Quantitative analysis of the depth of the defect was carried out. Through multiple simulations, the variation of the Bz amplitude and phase with the same width (5mm) of different depths (1mm, 2mm, 3mm and 4mm) with the detection point gradually away from the excitation coil was obtained. The simulation results are imported into MATLAB software, and the comparison of Bz amplitude and phase curve changes under different depth defects is obtained, as shown

in Figure 4. In order to facilitate the observation of the curve observation, the portion of the graph where the curve changes is enlarged.

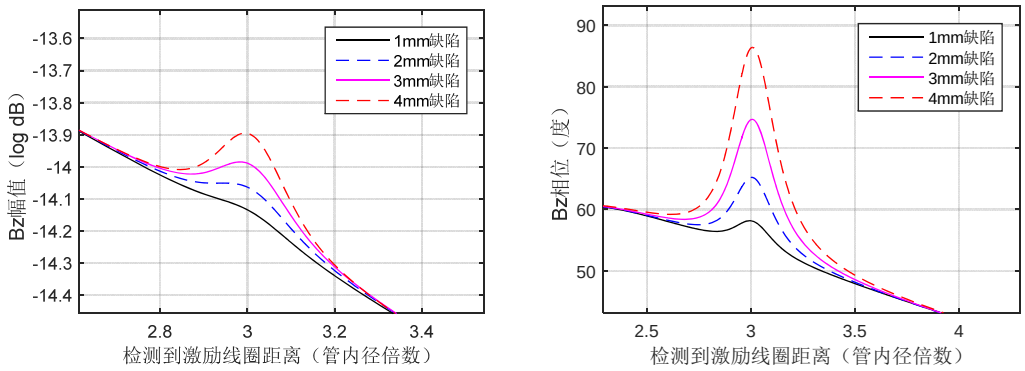

(a)Bz amplitude contrast curve (b)Bz phase contrast curve

Fig 6. Comparison of Bz amplitude and phase change curves under different depth defects

It can be seen from the comparison of the variation of Bz amplitude and phase curve under different depth defects in Figure 6. When the defect depth is different, the amplitude and phase curve of Bz change differently. The deeper the defect, the more obvious the curve changes. In the simulation model, the defect center is set at 3 times of the pipe diameter. It can also be found from the graph that the maximum point of the protrusion change is exactly 3 times the diameter of the defect center, regardless of the phase curve or the amplitude curve. In Figure 5(a), the magnitude of Bz amplitude is 10^{-14}, and the magnitude of the change is even only. This is difficult for the signal recognition of conventional equipment, which is easy to cause large errors. The noise signal easily covers the defect signal. The signal to noise ratio is very low. The variation of the Bz phase curve in Fig. 5(b) is between several degrees and several tens of degrees, and the range of variation is large, which can better distinguish whether there is a defect. Therefore, in the far field eddy current testing of pipeline defects, the change of the phase of the detection signal is more reliable as the main defect analysis signal, and the signal amplitude change can be used as the auxiliary analysis signal.

In order to further analyze the relationship between the depth of the defect and the magnetic field signal, the maximum value of the magnetic induction Bz phase protrusion at the center of the defect is extracted, and the phase of the corresponding depth defect is obtained by subtracting the phase from the defect without defect. The result is shown in the table. Figure 3 shows

Table 1. Change in Bz phase under different depth defects

Bz phase change	1mm	2mm	3mm	4mm
Phase change amount (degrees)	7.21	14.84	23.15	31.03

Drawing the data in Table 1 into a graph can more clearly show the relationship between the amount of phase change and the depth of the defect. The graph is shown in Figure 7. As can be seen from the figure, the phase change amount of the magnetic induction axial component Bz is substantially proportional to the depth of the defect. In the theoretical analysis part of Chapter 2, the phase of Bz and the phase of the induced voltage U of the detecting coil have a phase difference of 90 degrees. Therefore, the phase of the sense coil induced voltage U is also

proportional to the depth of the defect, whereby the defect can be detected and the depth of the defect can be roughly determined.

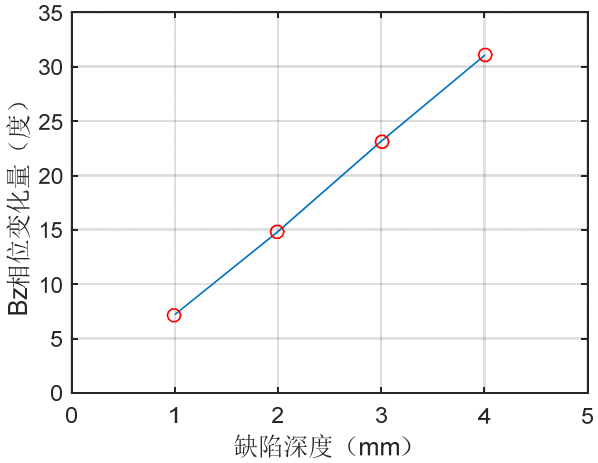

Fig 7. Bz phase change amount and defect depth relationship

3.3. Comparison of Internal and External Wall Defect Detection Simulation

In actual cases, defects may occur on the inner and outer walls of the pipe. For the same parameter defect, the defect center still takes 3 times the inner diameter of the distance excitation coil, the defect depth is 2mm, and the width is 5mm. The simulation is carried out for the defect in the outer wall of the pipe and the inner wall of the pipe, and a comparison chart of the amplitude and phase curve of Bz is obtained, as shown in Fig. 8 and Fig. 9. It can be seen from the two figures that when the same parameter defect exists in both the outer wall of the pipe and the inner wall of the pipe, the amplitude and phase curve of the axial component Bz of the magnetic induction intensity at the defect are basically coincident, and the amount of protrusion change is also the same. It can be seen that when far-field eddy current technology is used to detect the defect of the pipe wall, the sensitivity of the defect detection of the outer wall and the inner wall of the pipe is consistent. It is not necessary to analyze the inner wall defect of the pipe, and only the external wall defect is analyzed for the magnetic field signal and the detection coil voltage signal. The impact can be.

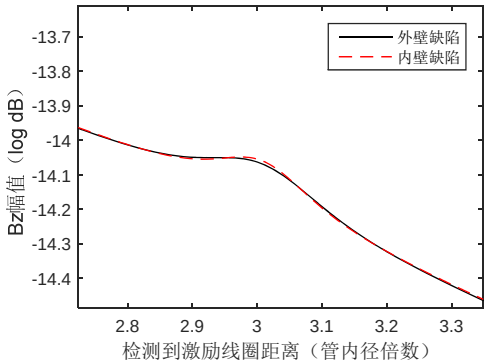

Fig 8. Bz amplitude contrast curve

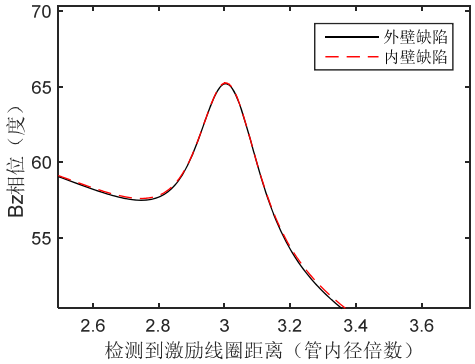

Fig 9. Bz phase contrast curve

4. Conclusion

In this paper, the far field eddy current technology is used to analyze the defect detection of oil and gas gathering pipelines. The theoretical knowledge of far field eddy current testing technology is expounded. On this basis, the full-circumferential axisymmetric defect detection simulation was carried out for ferromagnetic steel tubes. The distribution diagram of the magnetic field lines under the full circumferential axisymmetric groove defect is simulated, and the proportional relationship between the depth of the defect and the phase change of the

magnetic field signal is obtained. In addition, the effects of defects on the magnetic field signals in the inner and outer walls of the pipeline are compared, and the effect is the same. The conclusion that the far field eddy currents have the same sensitivity to the detection of the inner and outer wall defects of the pipeline is confirmed.

References

[1] Long K W. Study on Corrosion Mechanism and Anti Corrosion Technology of Oil and Gas Gathering and Transportation Pipeline[J]. Total Corrosion Control, 2017.

[2] Zhan-Kun L I, Sun B, Wang X L, et al. Corrosion Status Situation and Anti-corrosion Technology of Oil Gas Gathering and Distribution Pipelines in Tahe Oilfield[J]. Corrosion & Protection, 2015.

[3] Zi-Li L I, Sun Y F, Liu J, et al. Research Progress of AC Interference Corrosion and Protection of Buried Oil and Gas Pipelines[J]. Corrosion Science & Protection Technology, 2011, 23(5):376-380.

[4] Qin K, Zhu S. Application of X-ray Digital Radiography Technology in Steel Pipe Detection[J]. Welded Pipe & Tube, 2013.

[5] Chen X L, Chen P X, Chen X T, et al. Characteristics of pore pressure static cone penetration test parameters and its application of surface soil in pipeline laying areas[J]. Marine Sciences, 2012, 36(3):8-12.

[6] Haugland S M. Fundamental analysis of the remote-field eddy-current effect[J]. Magnetics IEEE Transactions on, 1996, 32(4):3195-3211.

[7] Schmidt T R. The Remote Field Eddy Current Inspection Technique[J]. Materials Evaluation, 1984, 42(2):225-230.

[8] Lord W, Sun Y S, Udpa S S, et al. A finite element study of the remote field eddy current phenomenon[J]. Magnetics IEEE Transactions on, 1988, 24(1):435-438.